**Advances and Applications in Statistics**

Published Online: November 2014
Available online at http://pphmj.com/journals/adas.htm
Volume 42, Number 1, 2014, Pages 65-82

# PARTIAL DIRECTED COHERENCE APPLICATIONS ON EEG DATA

**Kim Samejima M. Lopes**

Federal University of Bahia - UFBA
Av Adhemar de Barros, S/N, Ondina
40170-110 Salvador-BA
Brazil
e-mail: samejimal@ufba.br

## Abstract

This article is a review on multivariate time series relationship and its applications in electroencephalogram (EEG) data. We discussed the coherence function, an analogous function to the linear correlation function. We also studied partial coherence (PC) and partial directed coherence (PDC) functions. The PC function measures the relationship between two components of a multivariate time series when isolating effects of another series. Generally, PDC can be interpreted as the decomposition of partial coherence into multivariate autoregressive models, i.e., as a representation of Granger causality in the frequency domain. Finally, we applied those functions into EEG data from a subject in the resting state. Those functions are very interesting when we are interested not only on the correlation between time series, but also on the causality between them.

## 1. First Concepts

Let $\{X_t\}$ be a discrete and stationary time series with autocovariance

Received: July 12, 2014; Accepted: September 12, 2014
2010 Mathematics Subject Classification: 62-XX.
Keywords and phrases: time series, cross spectrum, coherence, partial coherence, partial directed coherence, EEG data.

function $\gamma_{XX}(u)$. If $\sum_{u=-\infty}^{\infty} |\gamma_{XX}(u)| < \infty$, then we have the *spectral density function*, or *spectrum* of $\{X_t\}$ defined by

$$f_{XX}(\omega) = \frac{1}{2\pi} \sum_{u=-\infty}^{\infty} \gamma_{XX}(u) e^{-i\omega u}, \quad -\pi < \omega < \pi. \tag{1}$$

Now, consider $I_{XX}^{(T)}(\omega)$ the periodogram of $\{X_0, ..., X_{T-1}\}$. Taking $s(T)$ an integer such that $2\pi s(T)/T$ is close to $\omega$, $I_{XX}^{(T)}$, $I_{XX}^{(T)}(2\pi[s(T) + j]/T)$, $j = 0, \pm 1, \pm 2, ..., \pm m$ are nearly independent. Then we have the *smoothed periodogram* defined by

$$f_{XX}^{(T)}(\omega) = m^{-1} \sum_{j=1}^{m} I_{XX}^{(T)}\left(\omega + \frac{2\pi j}{T}\right) \tag{2}$$

if $\omega = 0, \pm 2\pi, \pm 4\pi, ...$ and $T$ is even and

$$f_{XX}^{(T)}(\omega) = m^{-1} \sum_{j=1}^{m} I_{XX}^{(T)}\left(\omega - \frac{\pi}{T} + \frac{2\pi j}{T}\right) \tag{3}$$

with $\omega = \pm\pi, \pm 3\pi, ...$ and $T$ is odd.

Suppose now a vector $(X_t, Y_t)'$ weakly stationary.

*The cross covariance function* $\gamma_{XY}(k)$ is defined by

$$\gamma_{XY}(k) = \text{cov}(X_t, Y_{t+k}), \quad k = 0, \pm 1, \pm 2, .... \tag{4}$$

As well as the spectral density function, the *cross spectrum* (or *cross spectral density function*) is defined by the Fourier transform from the cross covariance function (4). So, supposing $\sum_k |\gamma_{XY}(k)| < \infty$, we define

$$f_{XY}(\omega) = \frac{1}{2\pi} \sum_{k=-\infty}^{\infty} \gamma_{XY}(k) e^{-i\omega k}, \quad -\pi < \omega < \pi. \tag{5}$$

As well as (3), we have $f_{XY}^{(T)}(\omega)$ the *smoothed cross periodogram* with *m-sized* windows.

## 2. Coherence Function

The *coherence function* is defined as

$$\kappa_{XY}^2(\omega) = \frac{|\, f_{XY}(\omega)|^2}{f_{XX}(\omega)\, f_{YY}(\omega)}. \tag{6}$$

The coherence function measures the quadratic correlation between two components in a bivariate process on the frequency (ω) and its analogous to the squared Pearson's linear correlation coefficient, but on the frequency domain.

A good coherence estimator is given as follows. As in the spectrum and cross spectrum estimation, the regular periodogram is not adequate, once the estimated coherence would have constant value 1. Then, since the quantities $f_{XX}^{(T)}(\omega)$, $f_{YY}^{(T)}(\omega)$ and $f_{XY}^{(T)}(\omega)$ are well defined and not zero, the ratio

$$\widehat{\kappa_{XY}^2(w)} = \frac{|\, f_{XY}^{(T)}(\omega)|^2}{f_{XX}^{(T)}(\omega)\, f_{YY}^{(T)}(\omega)} \tag{7}$$

is a good estimator for $\kappa_{XY}^2(\omega)$ on frequency ω.

It is known that:

$$E(\widehat{\kappa_{XY}(\omega)}) \approx \kappa_{XY}(\omega). \tag{8}$$

## 3. Partial Coherence

The *partial coherence* can be interpreted as a relationship (on frequency domain) between two components of a multivariate time series after removing the linear correlation of $\mathbf{X}(t)$ on $\mathbf{Y}(t)$. Consider a vector with length $(r + s)$, $r, s \in \mathbb{Z}$, compound by two multivariate time series $\mathbf{X}(t)$ and $\mathbf{Y}(t)$, $t \in \mathbb{Z}$, with lengths *r* and *s*, respectively,

$$\begin{bmatrix} \mathbf{X}(t) \\ \mathbf{Y}(t) \end{bmatrix}. \tag{9}$$

The residual time series of that approximation is

$$\boldsymbol{\varepsilon}(t) = \mathbf{Y}(t) - \mathbf{b}\sum_{u} \mathbf{a}(t-u)\mathbf{X}(u) \tag{10}$$

and **a** and **b** can be obtained by weighted least squares estimation (Brillinger [6]). So, if we consider the components **a** and **b** of $\mathbf{Y}(t)$, i.e., $Y_a(t)$ and $Y_b(t)$, we can estimate their *partial cross spectrum* after removing the effects of $\mathbf{X}(t)$ by considering the residuals defined above. On this way, if we consider the components **a** and **b** of $\varepsilon(t)$, $\varepsilon_a(t)$ and $\varepsilon_b(t)$, we can interpret their cross spectrum as the *partial cross spectrum* of $Y_a(t)$ and $Y_b(t)$. This *partial cross spectrum* can be calculated by

$$f_{Y_aY_b,\,X}(\omega) = f_{Y_a,\,Y_b}(\omega) - \mathbf{f}_{Y_a,\,X}(\omega)\mathbf{f}_{XX}(\omega)^{-1}\mathbf{f}_{X,\,Y_b}(\omega) = f_{\varepsilon_a,\,\varepsilon_b}(\omega). \tag{11}$$

The coherence between $\varepsilon_a(t)$ and $\varepsilon_b(t)$ represents the *partial coherence* between $Y_a(t)$ and $Y_b(t)$ after removing the $\mathbf{X}(t)$ effects and can be calculated by the following equation:

$$\mathbf{R}_{Y_aY_b,\,X}(\omega) = \frac{f_{Y_aY_b,\,X}(\omega)}{[f_{Y_aY_a,\,X}(\omega)\, f_{Y_bY_b,\,X}(\omega)]^{1/2}}. \tag{12}$$

**Estimation of $\mathbf{R}_{Y_aY_b,\,X}$**

Consider a vector of length $(r+s)$ represented by (9), $t = 0, ..., T-1$. We can calculate its *discrete Fourier transform* by

$$\begin{bmatrix} \mathbf{d}_X^{(T)}(\omega) \\ \mathbf{d}_Y^{(T)}(\omega) \end{bmatrix} = \sum_{t=0}^{T-1} e^{-i\omega t} \begin{bmatrix} \mathbf{X}(t) \\ \mathbf{Y}(t) \end{bmatrix}, \qquad \omega \in \mathbb{R}. \tag{13}$$

It is known (see Takahashi et al. [22]) that when $T \to \infty$ and $\omega \neq 0$, then (13) has asymptotic multivariate normal distribution:

$$\begin{bmatrix} \mathbf{d}_X^{(T)}(\omega) \\ \mathbf{d}_Y^{(T)}(\omega) \end{bmatrix} \sim N_{r+s}^{c}\left(0,\, 2\pi T \begin{bmatrix} \mathbf{f}_{XX}(\omega) & \mathbf{f}_{XY}(\omega) \\ \mathbf{f}_{YX}(\omega) & \mathbf{f}_{YY}(\omega) \end{bmatrix}\right). \tag{14}$$

We can now define the cross periodogram matrix, given by

$$\mathbf{I}_{XY}^{(T)}(\omega) = (2\pi T)^{-1}\mathbf{d}_X^{(T)}(\omega)(\overline{\mathbf{d}_Y^{(T)}(\omega)})^{\tau}, \tag{15}$$

and $\mathbf{I}_{XX}^{(T)}(\omega)$ and $\mathbf{I}_{YY}^{(T)}(\omega)$, defined similarly.

If we take $W^{(T)}(\alpha)$ a family of weights $2\pi$-periodic, $-\infty < \alpha < \infty$, $T = 1, 2, \ldots$, arranged in a reasonable way. Also consider $B_T > 0$, $B_T \to 0$, $B_T T \overset{T\to\infty}{\to} \infty$ a list of scale parameters and a function $W(\alpha)$ with the following properties:

$$\int_{-\infty}^{\infty} W(\alpha)d\alpha = 1, \qquad \int_{-\infty}^{\infty} |W(\alpha)|d\alpha < \infty.$$

Then we can construct $W^{(T)}(\alpha)$ by

$$W^{(T)}(\alpha) = \sum_{j=-\infty}^{\infty} B_T^{-1}W(B_T^{-1}[\alpha + 2\pi j]), \qquad -\infty < \alpha < \infty.$$

Finally, we can estimate the matrix

$$\mathbf{f}(\omega) = \begin{bmatrix} \mathbf{f}_{XX}(\omega) & \mathbf{f}_{XY}(\omega) \\ \mathbf{f}_{YX}(\omega) & \mathbf{f}_{YY}(\omega) \end{bmatrix} \tag{16}$$

by using the *smoothed cross periodogram matrix*

$$\mathbf{f}^{(T)}(\omega) = (2\pi T)^{-1}\sum_{s=0}^{T-1} W^{(T)}\left(\omega - \frac{2\pi s}{T}\right)\begin{bmatrix} \mathbf{I}_{XX}^{(T)}\left(\frac{2\pi s}{T}\right) & \mathbf{I}_{XY}^{(T)}\left(\frac{2\pi s}{T}\right) \\ \mathbf{I}_{YX}^{(T)}\left(\frac{2\pi s}{T}\right) & \mathbf{I}_{YY}^{(T)}\left(\frac{2\pi s}{T}\right) \end{bmatrix}$$

and the estimated *residual spectrum matrix* is given by

$$\mathbf{f}_{\varepsilon\varepsilon}^{(T)}(\omega) = \mathbf{f}_{YY}^{(T)}(\omega) - \mathbf{f}_{YX}^{(T)}(\omega)\mathbf{f}_{XX}^{(T)}(\omega)^{-1}\mathbf{f}_{XY}^{(T)}(\omega). \tag{17}$$

The *partial coherence estimator* is

$$\mathbf{R}_{Y_aY_b,X}^{(T)}(\omega) = \frac{f_{\varepsilon_a\varepsilon_b}^{(T)}(\omega)}{[f_{\varepsilon_a\varepsilon_a}^{(T)}(\omega)\, f_{\varepsilon_b\varepsilon_b}^{(T)}(\omega)]^{1/2}}. \tag{18}$$

The coherence and partial coherence have only suggestions of a synchrony behaviour between the time series. Considering this, Saito and Harashima [20] defined the idea of *directed coherence* as a function that not only measures the synchrony but also the functional connection between time series. In other words, The directed coherence estimates also the structural relationship of time series, decomposing their variability in aspects *feedforward* and *feedback*. Finally, thanks to Saito and Harashima's [20] discussion about *directed coherence* (*DC*), Baccalá and Sameshima [1] defined the *partial directed coherence* (*PDC*). The essential idea behind the PDC is decompose the partial coherence into autoregressive multivariate models. This concept can be interpreted by a Granger causality (see Granger [9]) in the frequency domain. Indeed, Takahashi et al. [22] show that there is a direct relation between existence Granger causality and PDC function.

Consider the spectrum and cross spectrum matrix

$$\mathbf{f}(\omega) = \begin{bmatrix} f_{11}(\omega) & f_{12}(\omega) & \cdots & f_{1N}(\omega) \\ \vdots & \vdots & \ddots & \vdots \\ f_{N1}(\omega) & f_{N2}(\omega) & \cdots & f_{NN}(\omega) \end{bmatrix}, \tag{19}$$

$f_{ij}(\omega), \quad i, j = 1, ..., N$ defined as (5). Then the matrix (19) can be decomposed like

$$\mathbf{f}(\omega) = \mathbf{H}(\omega)\mathbf{\Sigma}\mathbf{H}^{H}(\omega), \tag{20}$$

where $\mathbf{H}^{H}(.)$ represents a Hermitian Matrix $\mathbf{H}(.)$ and $\mathbf{\Sigma}$ is the covariance matrix $\{\gamma_{ij}, i, j = 1, ..., N\}$. In order to define the matrix $\mathbf{H}$, consider $X_1(t), ..., X_N(t)$ a conjoint stationary time series such that we have a good approximation by autoregressive models as it follows:

$$\begin{bmatrix} X_1(t) \\ \vdots \\ X_N(t) \end{bmatrix} = \sum_{r=1}^{p} \mathbf{A}_r \begin{bmatrix} X_1(t-r) \\ \vdots \\ X_N(t-r) \end{bmatrix} + \begin{bmatrix} w_1(t) \\ \vdots \\ w_N(t) \end{bmatrix}, \tag{21}$$

where $w_1(t), ..., w_N(t)$ are white noises.

The matrix $\mathbf{H}(\omega)$ is given by

$$\mathbf{H}(\omega) = \overline{\mathbf{A}}^{-1}(\omega) = (\mathbf{I} - \mathbf{A}(\omega))^{-1}, \tag{22}$$

$$\mathbf{A}(\omega) = \sum_{r=1}^{p} \mathbf{A}_r z^{-r}|_{z=e^{-i2\pi\omega}} = \sum_{r=1}^{p} \mathbf{A}_r e^{i2\pi\omega\tau}, \tag{23}$$

$$\mathbf{A}_r = \begin{bmatrix} a_{11}(r) & a_{12}(r) & \cdots & a_{1N}(r) \\ \vdots & \vdots & \ddots & \vdots \\ a_{N1}(r) & a_{N2}(r) & \cdots & a_{NN}(r) \end{bmatrix}, \tag{24}$$

where $a_{ij}(r)$ are the linear interaction coefficients of $x_j(t-r)$ and $x_i(t)$, $i,\ j = 1, ..., N$.

Now consider the partial coherence function defined in (12). We can represent it by using $A_r$ and $\mathbf{\Sigma}$ as it follows:

$$\mathbf{R}_{Y_iY_j,X}(\omega) = \frac{\overline{\mathbf{a}}_i^H(\omega)\mathbf{\Sigma}^{-1}\overline{\mathbf{a}}_j(\omega)}{\sqrt{(\overline{\mathbf{a}}_i^H(\omega)\mathbf{\Sigma}^{-1}\overline{\mathbf{a}}_i(\omega))(\overline{\mathbf{a}}_j^H(\omega)\mathbf{\Sigma}^{-1}\overline{\mathbf{a}}_j(\omega))}}, \tag{25}$$

with $\mathbf{\Sigma}$ representing the residual on the model (21) and $\overline{\mathbf{a}}_k(\omega)$ is the $k$ column of $\overline{\mathbf{A}}(\omega)$.

The *partial directed coherence factor* between two time series $X_i(t)$ and $X_j(t)$ is given by

$$\pi_{ij}(\omega) \coloneqq \frac{\overline{A}_{ij}(\omega)}{\sqrt{\overline{\mathbf{a}}_j^H(\omega)\mathbf{\Sigma}^{-1}\overline{\mathbf{a}}_j(\omega)}}, \tag{26}$$

$\overline{A}_{ij}(\omega)$ is the $i,j$th element of $\overline{\mathbf{A}}(\omega)$, $i,\ j = 1, ..., N$.

It is immediate from that definition that (25) can be rewritten as

$$\mathbf{R}_{Y_iY_j,X}(\omega) = \pi_i^H(\omega)\mathbf{\Sigma}^{-1}\pi_j(\omega), \tag{27}$$

$\pi_i(\omega) \coloneqq [\pi_{1i}(\omega), ..., \pi_{Ni}(\omega)]'$.

Because the denominator of (26) depends on $\mathbf{\Sigma}$, The PDC confuses the Granger causality and the *instantaneous* Granger causality. To avoid this effect, the formal definition of the PDC is

$$\overline{\pi}_{ij}(\omega) := \frac{\overline{A}_{ij}(\omega)}{\sqrt{\overline{\mathbf{a}}_j^H(\omega)\overline{\mathbf{a}}_j(\omega)}}, \tag{28}$$

which considers only the *non-instantaneous* Granger causality. Omitting $\mathbf{\Sigma}$ from (27), we focused our studies into the relation between the past values of $X_j(t)$ and the present and future values of $X_i(t)$.

Note that $\overline{A}_{ij}(\omega)$ still can be written by

$$\overline{A}_{ij}(\omega) = \begin{cases} 1 - \sum_{r=1}^{p} a_{ij}(r)e^{-i2\pi\omega r}, \text{ if } i = j, \\ -\sum_{r=1}^{p} a_{ij}(r)e^{-i2\pi\omega r}, \text{ c.c.} \end{cases} \tag{29}$$

Because of this representation, we say that (28) is the frequency-domain Granger causality. According to Takahashi et al. [22], this is because of the hypothesis of Granger causality can be verified if and only if $\overline{\pi}_{ij}(\omega) \equiv 0$ for all frequencies in the sampled range, $\omega \in [-0.5, 0.5]$.

## 4. Applications: EEG Data Analysis

From EEG data collected from an individual at resting state and eyes closed, with a sampling frequency of 250 Hz, we have the time series of EEG with the approximate length of 200,000 observations. Information from 32 different channels was collected, but in this article we describe only a few of them. The studied time series represent the differences of voltage between the sampling point of the electrode and the midpoint between the electrodes $P_z$ and $C_z$ shown in Figure 1.

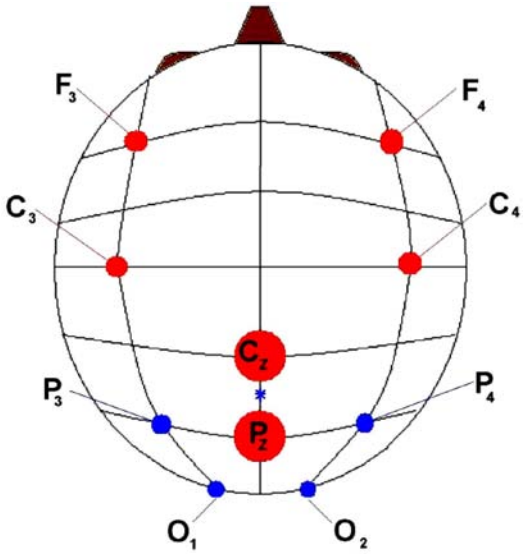


**Figure 1.** Position of electrodes for EEG.

We know, however, due to the high sampling frequency and the large amount of data, we can find problems such as long memory and non-stationarity in the study of EEG time series. Furthermore, in order to eliminate possible noise caused by measurement (involuntary thoughts of the patient, breathing, heartbeat, interference on the device, etc.), we chose to apply a bandpass-filter, with the filtering band between 1 and 100 Hz. Moreover, Bruscato [7] suggests the construction of spectrum estimators moving windows to avoid problems like global non-stationarity. For filtering, we use the `ffilter` function in the `seewave` package for the R software.

Thus, we construct estimates of the partial coherence function using moving windows throughout the time series, i.e., we construct the following multivariate vector:

$$\mathbf{R}^{(T)}_{J,Y_aY_b,X}(\omega) = [\mathbf{R}^{(T)}_{Y_aY_b,X}(\omega)|_{t\in(J_0=1,J_1)}, \ldots, \mathbf{R}^{(T)}_{Y_aY_b,X}(\omega)|_{t\in(J_{k-1},J_k)}, \ldots,$$

$$\mathbf{R}^{(T)}_{Y_aY_b,X}(\omega)|_{t\in(J_{K-1},J_{K=T})}]_{\left[\frac{M}{2}\right]\times K}, \tag{30}$$

$M$ is the window length, $\{(J_{k-1},\ J_{\kappa}),\ k = 1,\ ...,\ K\}$ is a set of embedded intervals,

$$\bigcup_{k=1}^{K}(J_{k-1},\ J_k) = (1,\ T)$$

and $K = \left[\frac{T}{M}\right]$ (biggest integer less than or equal to $\frac{T}{M}$).

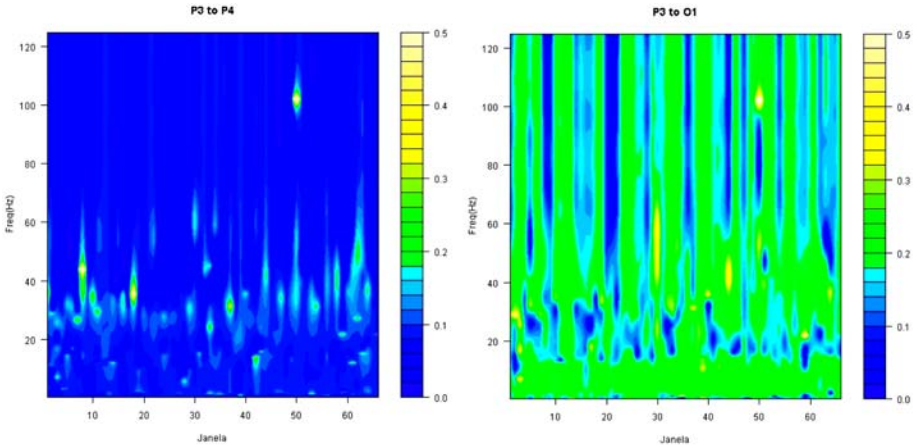


**Figure 2.** Partial coherence with moving window between $P3 \leftrightarrow P4$ and $P3 \leftrightarrow O1$.

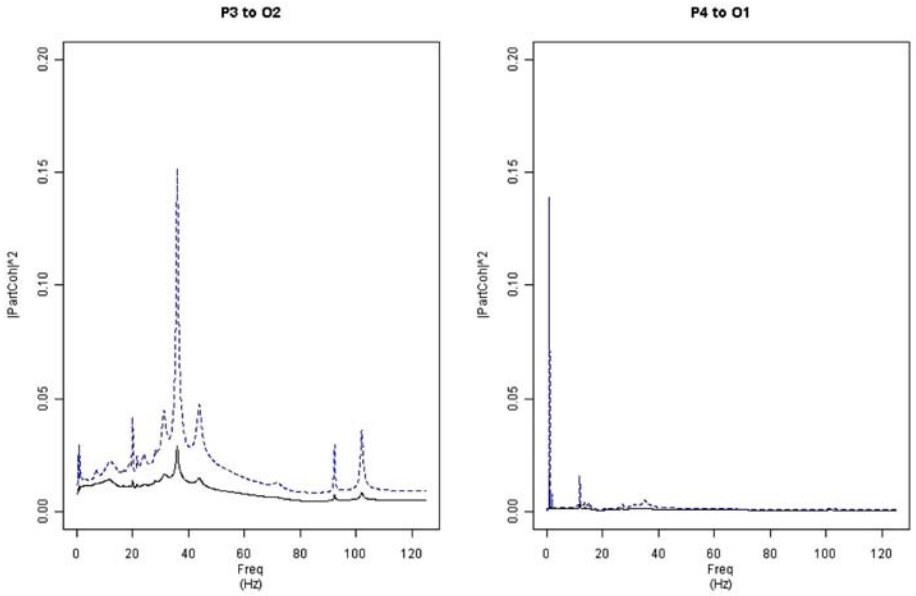


**Figure 3.** Mean curves for partial coherence with moving windows between P3 ↔ O2 and P4 ↔ O1. The black continuous line is the mean and the blue dashed line represents the standard deviation.

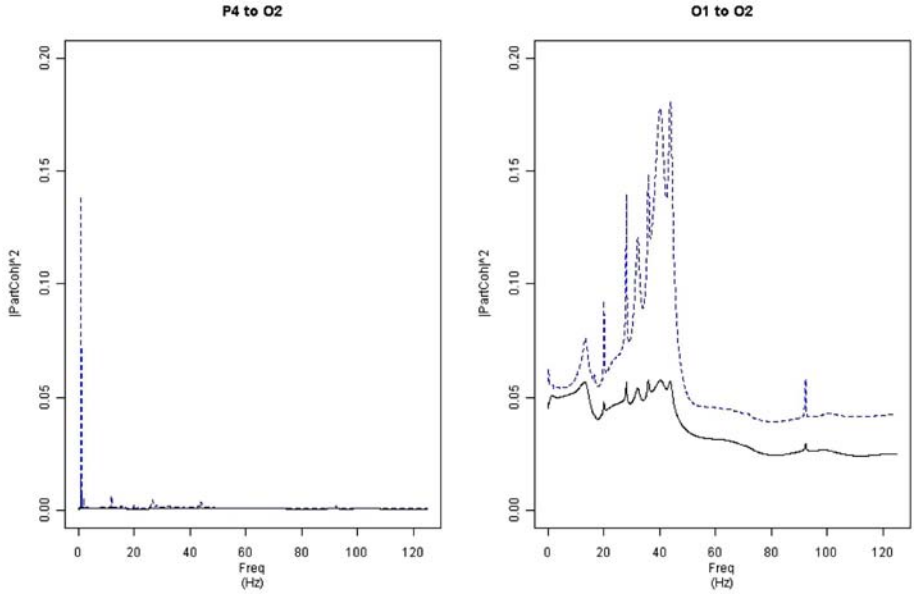


**Figure 4.** Mean curves for partial coherence with moving windows between P4 ↔ O2 and O1 ↔ O2.

In Figures 2 to 4, we can see graphs of $|\mathbf{R}^{(T)}_{J,Y_A Y_b,X}(\omega)|$ for some of the EEG time series with $M = 2000$. High activities relationships between the occipital channels were indeed expected, as described in Blinowska et al. [4]. If we analyze the mean curves, however, we see that in almost all partial coherence graphs, we found peaks of energy in higher frequencies: above 30 Hz, sometimes near 40 Hz, 55 Hz other near.

In medicine, it is common to analyze EEG data using frequency bands. In general, we can categorize the frequency in 5 bands: Gamma (frequencies greater than 30 Hz), Beta (13-30 Hz), Alpha (8-12 Hz), Theta (4-8 Hz), Delta (less than 4 Hz). Situations with less activity partial coherence found when we compared the relations $\mathrm{P4} \leftrightarrow \mathrm{Ol}$ and $\mathrm{P4} \leftrightarrow \mathrm{O2}$.

As well as the partial coherence functions, the partial directed coherence (PDC) functions are influenced by long memory and non-normality. Because of that, we also filtered the time series (same band) and build functions with windows with size 2000. Figures 5 and 7 show, for each pair of time series, the evolution of the squared of the partial directed coherence along the windows. The squares of the PDCs were plotted because we can interpret it as the percentage of information coming out of the time series of "origin" for the time series of "destiny." For the first group of channels, we see more "information exchange" occurring between channels $\mathrm{F3} \rightarrow \mathrm{C3}$, $\mathrm{F3} \rightarrow \mathrm{C4}$, $\mathrm{F4} \rightarrow \mathrm{C4}$, $\mathrm{F3} \rightarrow \mathrm{F4}$. In the group of occipital and parietal channels, we see more energy in PDCs $\mathrm{P3} \rightarrow \mathrm{P4}$ and $\mathrm{P3} \rightarrow \mathrm{O2}$.

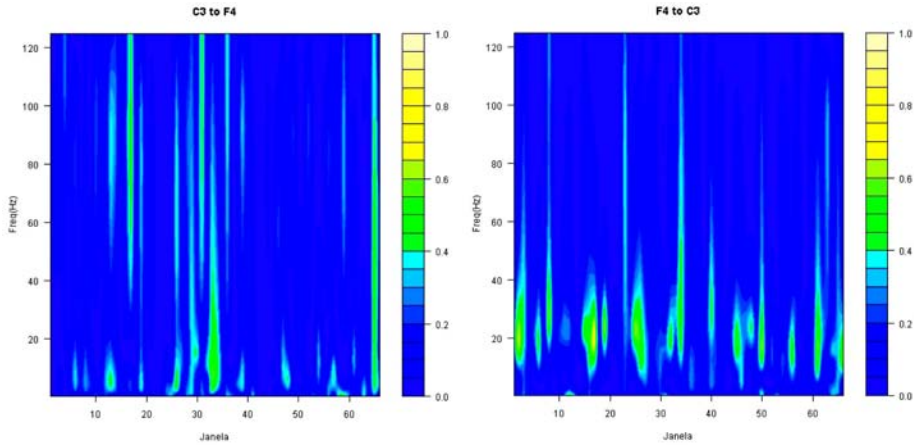


**Figure 5.** Partial coherence with moving windows between C3 and F4.

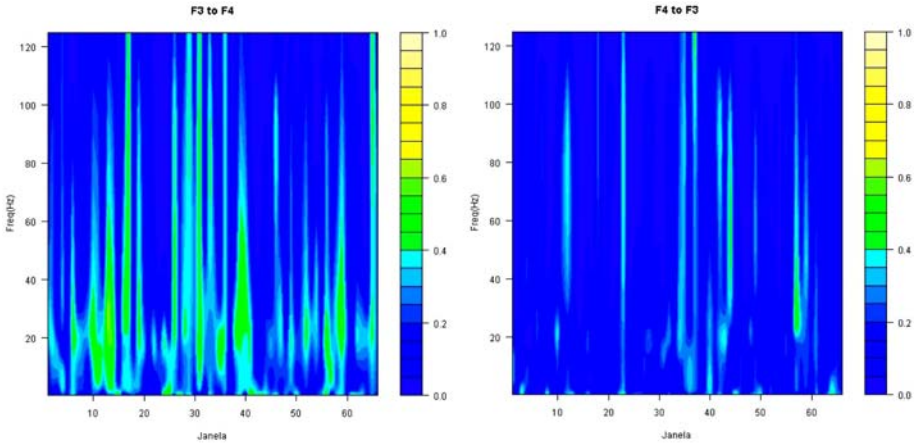


**Figure 6.** Partial directed coherence with moving windows between F3 and F4.

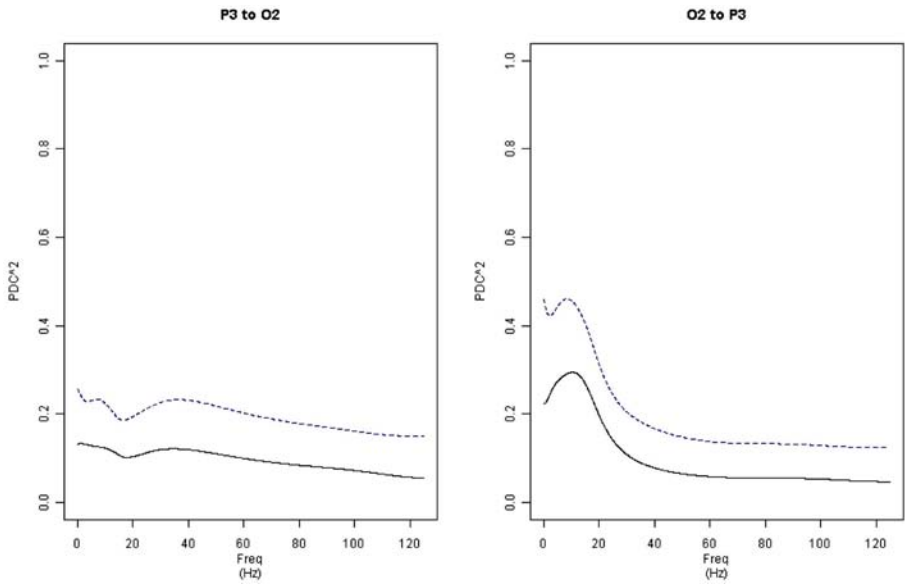


**Figure 7.** Partial coherence with moving windows between P3 and O2.

## 5. Results

Ginter et al. [8] and Biswal et al. [3] describe the relationship between movement areas (frontal lobes, F3 and F4) and central lobes (channels C3 and C4, for example) during movement tasks (or even in imaginary movements). We also can identify inter-hemisphere relations, as seen in F3 to F4 (Figure 6), also in Beta frequencies. Biswal et al. [3] and Heuvel et al. [11] also identified and described that kind of relation (in the medical perspective) considering data from *fMRI* (*functional Magnetic Resonance Imaging*).

From obtained results by measuring individuals in the same resting state, Kaplan and Shishkin [16] concluded by significant relationship between the electrode positions F3, F4, C3 and C4 as well as between electrodes at positions P3, P4, O1 and O2 evidencing two strong networks between those channels. Some different techniques can be used in order to evaluate that correlation. For example, Kaplan and Shishkin [16] compared the relationship between channels using nonparametric techniques (Wilcoxon paired test, $n = 12$).

We found similar relationships to those described by Kus et al. [17] between the parietal and occipital channels into Alpha frequency bands. Note that the *feedback* signal does not occur with the same intensity. These relationships between parietal and occipital channels (see Heuvel et al. [11]) are known in the literature as *core networks* and are those that control vision and sensory attention. The relations between regions back regions and medial-frontal regions, in other hand, are called *default mode networks* and control voluntary muscle movement, as described in Biswal et al. [3] and Ginter et al. [8].

There are still many relations between inter-hemisphere regions. In Figure 2, we find energy peaks on Beta and Gamma frequencies, considering the $P3 \leftrightarrow P4$ signal. If we consider the $P4 \leftrightarrow P3$ relationship, its peaks are concentrated around the Alpha and Beta frequencies. For occipital channels we identified higher concentration energy from O1 to O2 than from O1 to O2. Relations involving the occipital channels as a source of information generally show peaks at lower frequencies, typically in the Alpha frequencies.

## 6. Final Thoughts

The correlation and coherence functions were and are widely used to measure relationship between variables. However, there are many limitations when we are interested on interaction between variables. One of its limitations, for example, is evaluating in which direction flows the information. Sometimes, this makes it difficult to interpret the results, since there is no information about a possible causality between variables. Another limitation occurs when we consider that other variables may influence the relationship between the variables. This can lead to false conclusions about the relationship between the variables of interest (*spurious correlations*).

Directed coherence (Saito and Harashima [20]) and partial directed coherence functions, in other hand, can tell us not only about the mutual synchrony between time series, but also can measure influences from the first time series to the second and *vice versa*. Although not having a proven causal relationship when we apply the DC and PDC functions, we have the strong

suggestions that this relationship does exist. We may, from there, build and testing of hypotheses to evaluate the relationship between the variables (see Takahashi et al. [22]).

Still further, assuming that our multivariate process to be a **VAR** of finite order, computational aspects benefits the PDC if compared to DC function, since the matrix $\mathbf{H}(.)$ given in (22) need not be calculated for each frequency of interest. The fact of PDC is non-dependent on this matrix $\mathbf{H}(.)$ implies a greater stability of the calculated function (from the computational perspective), since the coefficient matrix inversion can present singularity problems, for example, when considering small samples. Another good quality of the PDC is the fact of eliminate the influences of another time series, isolating only the influences we are interested on. However, this is not valid if we have moving average multivariate process (i.e., a **VARMA** with null autoregressive coefficients), since its representation occurs with an infinite order **VAR**.

Another way to estimate the relationship between multivariate time series can be made using *wavelet analysis*. Percival and Walden [18] discuss the methodology applied on measurement the relationship between time series. Torrence and Compo [25] present a practical guide to wavelet applications in studies of multivariate time series. Other wavelet applications in the study of interactions in time series can be viewed on Torrence and Webster [24] and Grinsted et al. [10].

## References

[1] L. A. Baccalá and K. Sameshima, Partial directed coherence: a new concept in neural structure determination, Biological Cybernetics 84 (2001), 463-474.

[2] L. A. Baccalá, K. Sameshima and D. Y. Takahashi, Computer intensive testing for influence between time series, Handbook of Time Series Analysis, 1, 2006.

[3] B. Biswal, F. Z. Yetkin, V. M. Haughton and J. S. Hyde, Functional connectivity in the motor cortex of resting human brain using echo-planar MRI, Magn. Reson. Med. 34 (1995), 537-541.

[4] K. J. Blinowska, R. Kuś and M. Kamiński, Granger causality and information flow in multivariate processes, Phys. Rev. E 70 (2004), 050902(R).

[5] K. J. Blinowska, M. Kaminski, R. Kus and J. Ginter, Transmission of brain activity in cognitive and motor tasks, 30th Annual International Conference of the IEEE, Engineering in Medicine and Biology Society, EMBS 2008, pp. 3508-3511.

[6] D. R. Brillinger, Time Series: Data Analysis and Theory, Expanded Ed., Holt, Rinehart and Winston, New York, 2001.

[7] A. Bruscato, Análise Espectral de Processos Não-Estacionários Utilizando a Transformada de Fourier, Dissertação de Mestrado, São Paulo: IME, 2000.

[8] J. Ginter, Jr., K. J. Blinowska, M. Kamiński, P. J. Durka, G. Pfurtscheller and C. Neuper, Propagation of EEG activity in the beta and gamma band during movement imagery in humans, Methods Inform. Med. 44(1) (2005), 106-113.

[9] C. W. J. Granger, Investigating causal relations by econometric models and cross-spectral methods, Econometrica 37(3) (1969), 424-438.

[10] A. Grinsted, J. C. Moore and S. Jevrejeva, Application of the cross wavelet transform and wavelet coherence to geophysical time series, Nonlinear Processes in Geophysics 11 (2004), 561-566.

[11] M. P. van den Heuvel, R. C. W. Mandl, R. S. Kahn and H. E. Hulshoff Pol, Functionally linked resting-state networks reflect the underlying structural connectivity architecture of the human brain, Human Brain Mapping 30(10) (2009), 3127-3141.

[12] M. Kaminski and K. J. Blinowska, A new method of the description of the information flow, Biological Cybernetics 65 (1991), 203-210.

[13] M. Kaminski, M. Ding, W. A. Truccolo and S. T. Bressler, Evaluating casual relations in neural systems: Granger causality, directed transfer function and statistical assessment of significance, Biological Cybernetics 85 (2001), 145-157.

[14] M. Kaminski, Determination of transmission patterns in multichannel data, Phil. Trans. Royal Soc. 360 (2005), 947-952.

[15] M. Kaminski, J. Zygierewicz, R. Kus and N. Crone, Analysis of multichannel biomedical data, Acta. Neurobiol. Exp. (Wars) 65 (2005), 443-452.

[16] A. Ya. Kaplan and S. L. Shishkin, Application of the change-point analysis to the investigation of the brain's electrical activity, Nonparametric Statistical Diagnosis: Problems and Methods, Kluwer Academic Publishers, Dordrecht, The Netherlands, 2000, pp. 333-388.

[17] R. Kus, M. Kaminski and K. J. Blinowska, Determination of EEG activity propagation: pair-wise versus multichannel estimate, IEEE Trans. Biomed. Eng. 51(9) (2004), 1501-1510.

[18] D. B. Percival and A. T. Walden, Wavelet Methods for Time Series Analysis, Cambridge University Press, New York, 2000.

[19] D. B. Percival and A. T. Walden, Spectral Analysis for Physical Applications: Multitaper and Conventional Univariate Techniques, Cambridge University Press, New York, 1993.

[20] Y. Saito and H. Harashima, Tracking of information within multichannel EEG record – causal analysis in EEG, Recent Advances in EEG and EMG Data Processing, Elsevier, Amsterdam, 1981, pp. 133-146.

[21] J. R. Sato, D. Y. Takahashi, S. M. Arcuri, L. A. Baccalá, P. A. Morettin and K. Sameshima, Frequency domain connectivity identification: an application of partial directed coherence in fMRI, Human Brain Mapping 30 (2009), 452-461.

[22] D. Y. Takahashi, L. A. Baccalá, K. Sameshima, Connectivity inference via partial directed coherence: asymptotic results, J. Appl. Stat. 34 (2007), 1259-1273.

[23] D. Y. Takahashi, L. A. Baccalá and K. Sameshima, On partial directed coherence factor, Granger causality and information theory, 10th Tamagawa-Riken Brain Dynamics Brain Forum - DBF07, 2007a.

[24] C. Torrence and P. J. Webster, Interdecadal changes in the ENSO - monsoon system, J. Climate 12 (1999), 2679-2690.

[25] C. Torrence and G. P. Compo, A practical guide to wavelet analysis, Bull. Amer. Meteorol. Soc. 79 (1998), 61-78.

[26] O. Yamashita, N. Sadato, T. Okada and T. Ozaki, Evaluating frequency-wise directed connectivity of BOLD signals applying relative power contribution with linear multivariate time-series models, NeuroImage 25 (2005), 478-490.